LAPCs promote follicular helper T cell differentiation of Ag-primed CD4+ T cells during respiratory virus infection

Jae-Kwang Yoo,[1] Eleanor N. Fish,[4] and Thomas J. Braciale[1,2,3]

[1]Beirne B. Carter Center for Immunology Research, [2]Department of Microbiology, and [3]Department of Pathology, University of Virginia, Charlottesville, VA 22908
[4]Toronto General Research Institute, University Health Network, Toronto, Ontario M5G 2M1, Canada

The humoral immune response to most respiratory virus infections plays a prominent role in virus clearance and is essential for resistance to reinfection. T follicular helper (Tfh) cells are believed to support the development both of a potent primary antibody response and of the germinal center response critical for memory B cell development. Using a model of primary murine influenza A virus (IAV) infection, we demonstrate that a novel late activator antigen-presenting cell (LAPC) promotes the Tfh response in the draining lymph nodes (dLNs) of the IAV-infected lungs. LAPCs migrate from the infected lungs to the dLN "late," i.e., 6 d after infection, which is concomitant with Tfh differentiation. LAPC migration is CXCR3-dependent, and LAPC triggering of Tfh cell development requires ICOS–ICOSL–dependent signaling. LAPCs appear to play a pivotal role in driving Tfh differentiation of Ag-primed CD4+ T cells and antiviral antibody responses.

CORRESPONDENCE
T. J. Braciale:
tjb2r@virginia.edu

Abbreviation used: Ab, antibody; Ag, antigen; BAL, bronchoalveolar lavage; dLN, draining LN; dpi, days postinfection; GC, germinal center; IAV, influenza A virus; LAPC, late activator APC; Tfh, follicular helper T cell; Tg, transgenic.

The host adaptive immune response plays a central role in recovery from virus infection and resistance to reinfection. In the case of respiratory virus infection, the orchestration of an effective B cell response with the production of neutralizing antibodies is not only essential to preventing reinfection, but is also critical for the ultimate elimination of infectious virions from the respiratory tract after primary virus infection (Graham and Braciale, 1997; Waffarn and Baumgarth, 2011).

When analyzed in detail in experimental models, the antibody response to primary respiratory virus infection consists of contributions from innate-like B-1 B cells, as well as virus-specific adaptive B cells localized to the extrafollicular (marginal zone) and follicular regions of the lymphoid tissue e.g., LNs draining the sites of infection (Waffarn and Baumgarth, 2011). Upon secondary exposure to virus, B cells present in inflammation-induced bronchial-associated lymphoid tissue can also provide a local contribution to this antibody response. After activation by antigen, adaptive B cells undergo proliferative expansion and a series of differentiation events, resulting in the formation of germinal centers (GCs) within the lymphoid follicles, where antigen receptor affinity maturation and memory B cell formation occur (Vinuesa et al., 2005; Linterman and Vinuesa, 2010). The effective activation and differentiation of both extrafollicular and follicular B cells have been demonstrated both for model protein antigens and, more recently, after virus infection, to be dependent on CD4+ T cell help (Vogelzang et al., 2008; Nurieva et al., 2008; Lee et al., 2011; Choi et al., 2011).

A distinct subpopulation of CD4+ T cells, T follicular helper (Tfh) cells, have been implicated as the major provider of T cell help for B cell activation/differentiation and, particularly from studies both in humans and rodents, for the GC response and the generation of GC B cells (Breitfeld et al., 2000; Schaerli et al., 2000; Kim et al., 2001; Crotty, 2011; Morita et al., 2011). Tfh cells express distinct cell surface markers, e.g., PD-1+CXCR5+, transcription factors, e.g., Bcl-6, and characteristic cytokines, e.g., IL-4 and IL-21. Whether Tfh cells represent a unique CD4+ T cell subset or simply reflect an activation state of the effector CD4+

The Rockefeller University Press $30.00
J. Exp. Med. 2012 Vol. 209 No. 10 1853-1867
www.jem.org/cgi/doi/10.1084/jem.20112256

T cells, is unclear. Although Tfh cells can drive B cell differentiation and GC formation through the combination of release of soluble mediators (IL-4 and IL-21) and co-stimulatory ligand–receptor interactions (CD40–CD40L and ICOS–ICOSL; Crotty, 2011), the factors regulating the generation of Tfh cells from naive $CD4^+$ precursors remain to be fully elucidated.

Recently, we identified a novel $CD45^+$ mononuclear cell type present in virus-infected murine lungs. This cell type migrates from the lungs to the draining lymph nodes (dLNs) late in the infection cycle, i.e., between 6 and 12 d postinfection (dpi; Yoo et al., 2010a,b). This late activator APC (LAPC) subset is distinct from conventional DCs. Upon migration to the dLN, LAPCs were shown to support TH2-type $CD4^+$ T cell differentiation and, importantly, to enhance antiviral antibody responses. These properties of LAPCs identify them as attractive candidates to serve as regulators of Tfh differentiation during respiratory virus infection. In this work, we demonstrate that LAPCs act as key regulators for Tfh differentiation of Ag-primed $CD4^+$ T cells during IAV infection.

RESULTS

$CD4^+$ Tfh differentiation during IAV infection

To better characterize the helper T cell response to virus infection at a peripheral (mucosal) site, i.e., the lungs, we examined the kinetics of antiinfluenza Tfh T cell generation and accumulation in the dLN after primary IAV infection. BALB/c mice were infected intranasally (i.n.) with a sublethal dose (0.05 LD_{50}) of A/PR/8 (H1N1) virus, and the generation of Tfh T cells was monitored in the dLN by PD-1 and CXCR5 co-staining. Tfh T cells were first detected between 3 and 6 dpi, and the accumulation of these polyclonal Tfh T cells reached a peak at 12 dpi, both in terms of absolute T cell numbers and their percentage relative to other cell subsets (Fig. 1 a). Comparable kinetics of Tfh accumulation were observed in infected C57BL/6 mice (unpublished data).

The GC B cell response is regulated in a Tfh-dependent manner (Vinuesa et al., 2005). During i.n. IAV infection, we first detected a GC B cell ($B220^+Fas^+GL\text{-}7^+$) response in the dLN at 6 dpi; the response reached a peak at 12 dpi (Fig. 1 a) and had kinetics analogous to that of Tfh cells. However, this GC B cell response was sustained (at least 20 dpi), despite contraction of the Tfh response.

The kinetics of Tfh accumulation were further verified in experiments using influenza hemagglutinin (H1-HA) specific TcR transgenic (Tg) $CD4^+$ (TS-1) T cells (Sun et al., 2011). For this, TS-1 cells were isolated from naive $Thy1.1^+$ TS-1 mice and transferred by the i.v. route into Thy-1 mismatched BALB/c mice. 24 h later, mice were infected i.n. with A/PR/8 virus and Tfh accumulation was monitored in the dLN by PD-1 and CXCR5 co-staining. The kinetics of accumulation of the TcR Tg TS-1 Tfh cells paralleled the response of polyclonal $CD4^+$ T cells (Fig. 1 b). Unexpectedly, although the majority (>95%) of in vivo Ag-primed TS-1 in the dLN when analyzed up to 5 dpi displayed an activated ($CD44^{hi}$ or $CD62L^{lo}$) phenotype relative to naive TS-1 (Fig. 1 c), we failed to detect a significant number of TS-1 T cells coexpressing the characteristic Tfh cell markers PD-1 and CXCR5 up to 5 dpi Therefore, the rate of Tfh cell differentiation was delayed relative to the activation and initial proliferation of naive virus-specific $CD4^+$ T cells (Legge and Braciale, 2003; Kim and Braciale, 2009). This finding raised the possibility that factors other than the initial encounter of naive $CD4^+$ T cells with migrant respiratory DCs within the dLN at 2–3 dpi may influence Tfh cell differentiation in the dLN after respiratory virus infection.

IAV-activated LAPCs promote Tfh differentiation of Ag-primed $CD4^+$ T cells ex vivo

Unlike conventional APCs, such as respiratory DCs, LAPCs migrate from the infected respiratory tract to the dLN late in IAV infection, i.e., 6 dpi and later (Fig. 1 a). Because the kinetics of LAPC accumulation in the dLN paralleled Tfh generation/accumulation, we sought to determine if migrant LAPCs within the dLN can influence Tfh differentiation. Accordingly, we analyzed the effect of co-culture of LAPCs with in vivo–activated, IAV-specific TS-1 T cells isolated from the dLN before Tfh differentiation, at 5 dpi. In brief, the isolated TS-1 T cells were cultured for 24 h with either B cells ($B220^+CD19^+CD11c^-$), activated B cells ($B220^+CD19^+CD69^+CD11c^-$), DCs ($CD11c^+TcR\beta^-$), or LAPCs ($mPDCA1^+CD11c^-B220^-TcR\beta^-$) isolated from the dLN on 8 dpi, as both DCs and B cells have been implicated as critical regulators of Tfh differentiation (Nurieva et al., 2008; Choi et al., 2011). To address the requirement for specific antigen recognition for Tfh differentiation, these APC populations were isolated from the dLN of either A/PR/8 virus–infected mice or mice infected with the X31(H3N1) influenza strain, whose hemagglutinin (H3-HA) is not recognized by TS-1 T cells. During the last 4 h of incubation, cells were treated with GolgiStop to examine cytokine production. Tfh differentiation and cytokine production by cultured TS-1 were monitored by FACS analysis (Fig. 2 a).

As shown in Fig. 1 c, in vivo Ag-primed TS-1 cells when isolated 5 dpi, displayed an activated phenotype compared with naive TS-1 cells, including elevated expression of PD-1, but did not display the PD-1 and CXCR5 double-positive co-staining characteristic of Tfh T cells. We found that B cells, even if selected for an activated phenotype ($B220^+CD19^+CD69^+CD11c^-$), were extremely poor inducers of Tfh differentiation in this short-term ex vivo co-culture setting. We confirmed that this was not caused by a loss of viability of ex vivo co-cultured B cells, as only a modest decrease in live B cells, both total and activated B cells, was observed over 24 h of co-culture with T cells (3–9% death; unpublished data). DCs did induce a modest increase in PD-1 and CXCR5 double-positive cell numbers after co-culture with in vivo Ag-primed TS-1. In contrast, interaction of activated TS-1 cells with LAPCs resulted in a larger increase in the development of PD-1 and CXCR5 double-positive Tfh cells in culture (Fig. 2 b). Notably, in this setting of ex vivo co-culture, Tfh differentiation was not dependent on specific antigen recognition

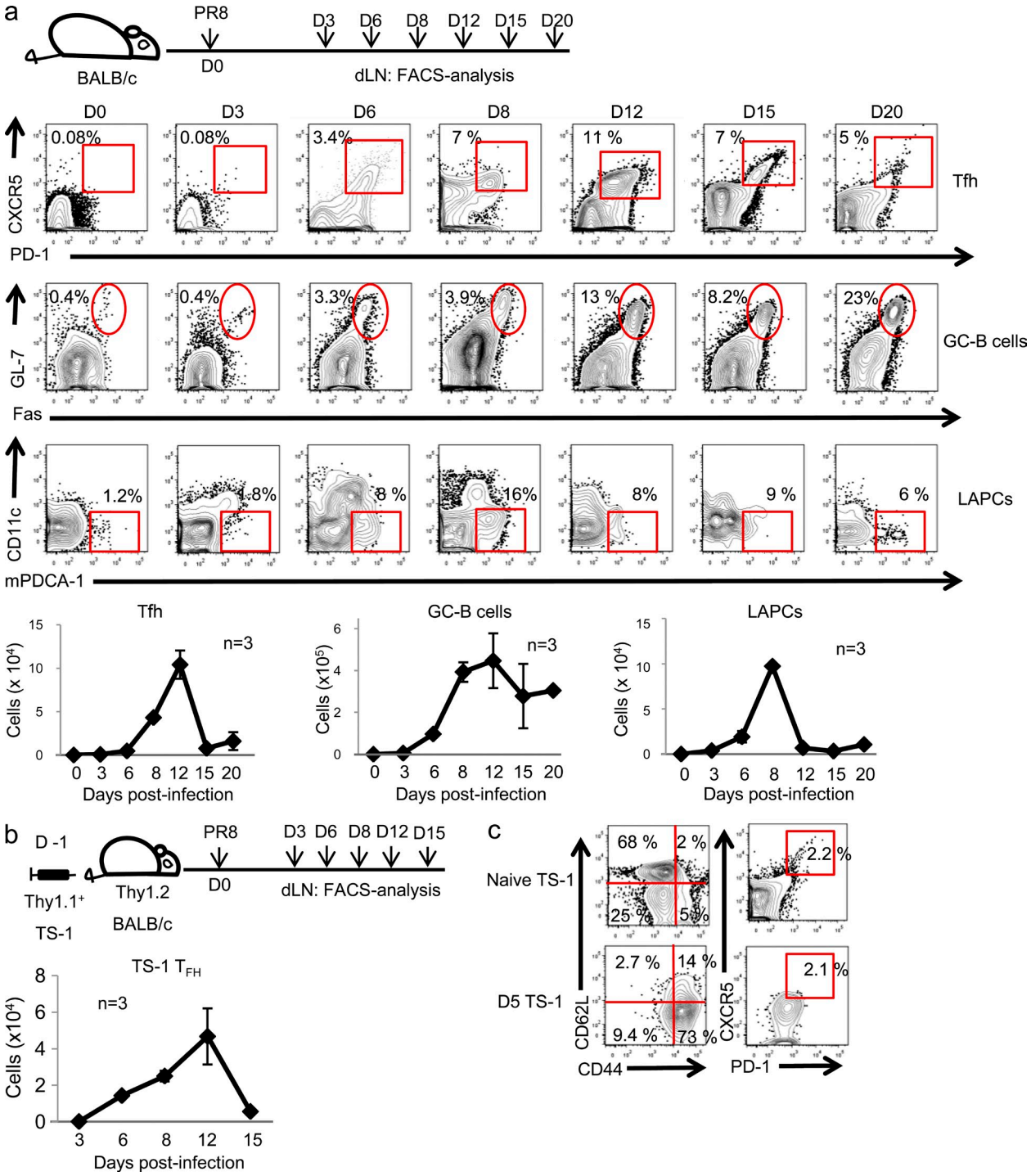

Figure 1. The kinetics of Tfh and GC B cell responses correlate with LAPC migration into the dLNs in IAV infection. (a) BALB/c mice (n = 42) were infected intranasally (i.n.) with a sublethal dose (0.05 LD_{50}) of A/PR/8 virus, as described in Materials and methods. At the indicated days after infection, the extent of Tfh (Thy1.2$^+$CD4$^+$PD-1$^+$CXCR5$^+$), GC B cell (B220$^+$Fas$^+$GL-7$^+$) and LAPC (mPDCA1$^+$CD11c$^-$B220$^-$TcRβ^-) responses were determined in the dLNs by FACS analysis. The data are presented as both percent population and absolute numbers (mean ± SEM). Representative stainings from at least three independent experiments are shown. (b) Naive TS-1 cells (Thy1.1$^+$CD4$^+$) were adoptively transferred into Thy1.2$^+$ BALB/c mice (n = 30) by i.v. injection. 24 h after transfer, mice were infected (i.n.) with a sublethal dose (0.05 LD50) of A/PR/8 virus. At the indicated dpi, dLNs were harvested and the extent of the Tfh response of transferred TS-1 cells (Thy1.1$^+$CD4$^+$PD-1$^+$CXCR5$^+$) was determined by FACS analysis. The data are presented as absolute numbers (mean ± SEM) in the dLNs. Representative data from two independent experiments are shown. (c) On 5 dpi, both the extent of activation (CD62L and CD44) and Tfh differentiation status (PD-1 and CXCR5) of TS-1 cells were evaluated by comparison with naive TS-1 cells, using FACS analysis. Representative images from two independent experiments are shown.

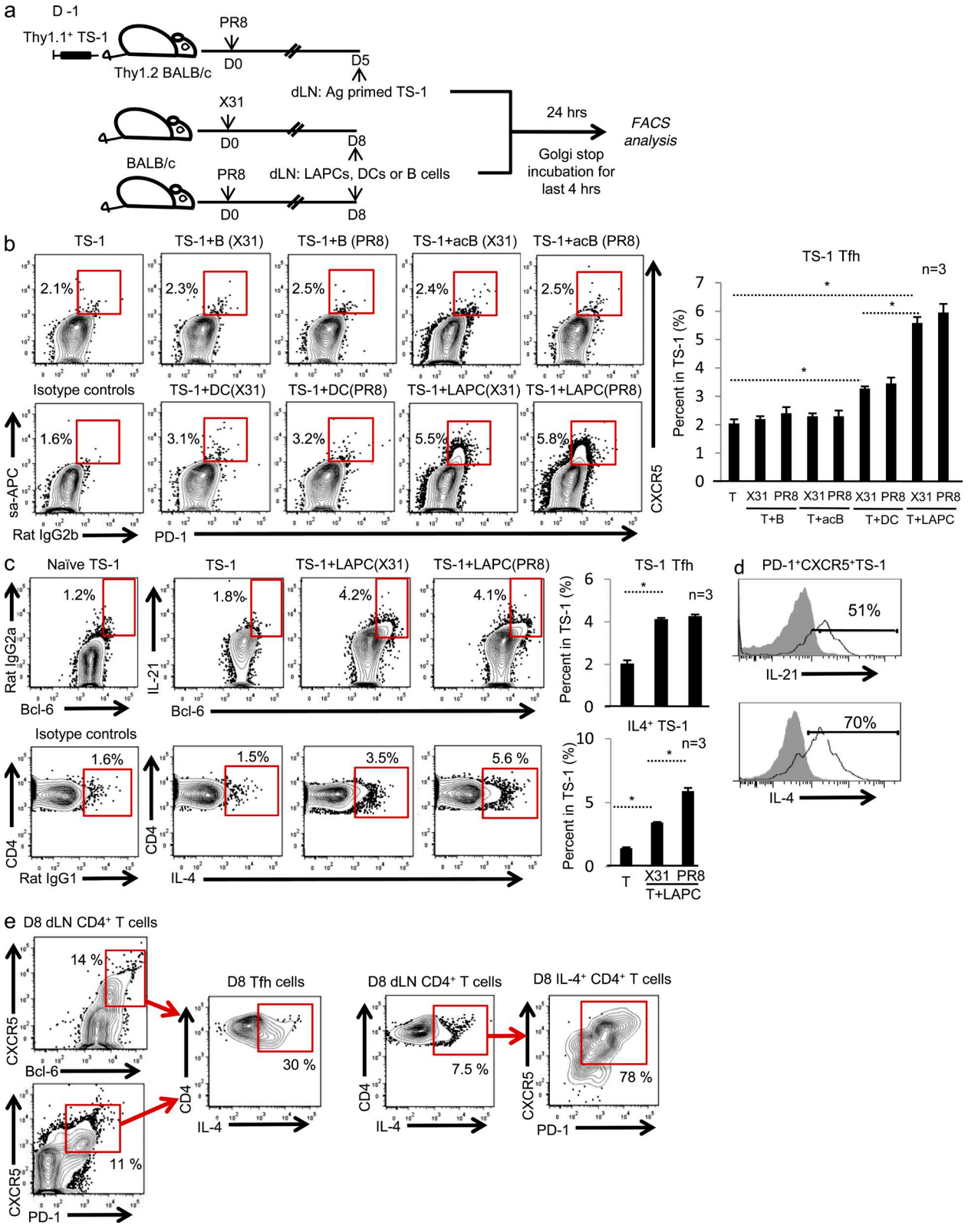

Figure 2. LAPCs promote IL-4+ type-2 Tfh differentiation of Ag-primed CD4+ T cells ex vivo. (a) Schematic diagram for ex vivo co-culture experiments. In vivo Ag-primed TS-1 cells were generated as described in Materials and methods. FACS-sorted 5 dpi TS-1 cells (5×10^4 cells/well) were incubated with either total B cells (B; $B220^+CD19^+CD11c^-$), activated B cells (acB; $B220^+CD19^+CD69^+CD11c^-$), DCs ($CD11c^+TcR\beta^-$) or LAPCs ($mPDCA1^+CD11c^-B220^-TcR\beta^-$; 2.5×10^4 cells/well) isolated from the dLN of either X31($n = 8$) or A/PR/8 virus-infected ($n = 8$) BALB/c mice on 8 dpi (b–d).

by the CD4+ T cells, as TS-1 cells co-cultured with either X31 or A/PR/8 virus–activated LAPCs differentiated into PD-1 and CXCR5 double-positive cells to a comparable extent. The expression of the Tfh differentiation transcriptional regulator, Bcl-6, and the signature Tfh effector cytokine, IL-21, were likewise up-regulated in an antigen-independent manner by IAV-activated LAPCs (Fig. 2, c and d).

LAPCs activated by virus infection (e.g., IAV) have previously been shown to stimulate IL-4 production by in vivo Ag-primed CD4+ T cells (Yoo et al., 2010b). IL-4 secretion by Tfh T cells is critical, supporting the GC B cell survival and isotype-switching (Yusuf et al., 2010; Crotty, 2011). We found that after co-culture with LAPCs, IL-4 was produced by the majority of PD-1+CXCR5+ TS-1 cells (70%; Fig. 2 d). Likewise, >75% of IL-4+CD4+ T cells from the dLN of influenza-infected mice exhibited a Tfh phenotype (PD-1+ CXCR5+) 8 dpi (Fig. 2 e). However, in contrast to LAPC-mediated induction of PD-1+CXCR5+ coexpression, or Bcl-6 and IL-21 up-regulation, the induction of IL-4 expression was statistically significantly augmented by specific antigen recognition because LAPCs from mice infected with A/PR/8 virus (recognized by the TS-1 TcR Tg T cells) were the most potent inducer of this cytokine (Fig. 2c).

ICOS–ICOSL interaction is critical for LAPC-mediated Tfh differentiation

To define the nature of the interaction between LAPCs and activated CD4+ T cells which promotes Tfh differentiation of Ag-primed CD4+ T cells, we first assessed the requirement for cell–cell contact in this process. When LAPCs and activated T cells were separated by a 0.4-μm membrane in trans-well cultures, LAPCs failed to drive Tfh differentiation (Fig. 3 a). In contrast, LAPCs could support Tfh differentiation in mixed cultures with T cells, even when LAPCs are exposed to high-level ionizing radiation (2,000 rads of gamma irradiation) before culture with activated T cells to suppress mediator release. These results suggested that this differentiation process requires direct contact between LAPCs and the activated T cells.

Because ICOS–ICOSL interactions have been implicated as critical in Tfh development (Nurieva et al., 2008; King and Mohrs, 2009; Choi et al., 2011; Kadkhoda et al., 2011), we evaluated the role of this co-stimulatory receptor/ligand pair in orchestrating LAPC-mediated Tfh differentiation. ICOS was abundantly expressed on the surface of activated TS-1 T cells at 5 dpi, and, although detected at a lower level and frequency, ICOSL was readily demonstrable on the surface of the corresponding LAPCs from infected mice (Fig. 3 b). When the ICOS–ICOSL interaction was inhibited by blocking antibody treatment in LAPC-T cell co-cultures, the blockade completely abolished the Tfh differentiation of activated TS-1 T cells, as determined by Tfh cell surface marker expression and also resulted in markedly diminished IL-4 production by the activated TS-1 T cells (Fig. 3 c).

LAPCs promote Tfh differentiation of Ag-primed CD4+ T cells via ICOS stimulation in the dLNs of IAV-infected mice

To more directly examine the role LAPCs in anti-IAV Tfh differentiation in the LN microenvironment during infection, ex vivo LN organ culture experiments were conducted.

LAPCs were originally identified as a novel APC population migrating from infected lung tissue into the dLN relatively late after i.n. IAV infection with the relatively attenuated mouse adapted A/WSN/33 IAV strain. To confirm the lung origin of LAPCs in the dLN and to establish the kinetics of LAPC migration and accumulation in the dLN after infection, we undertook infection experiments with the more virulent mouse adapted A/PR/8 IAV strain. The data revealed that few LAPCs were found in the dLN at 5 dpi with A/PR/8 IAV strain. LAPC accumulation was detected in the dLN from 6 dpi (Fig. 4 a). In parallel, FITC-dextran was delivered by the i.n. route to A/PR/8-infected mice at 5 dpi. 24 h later, LAPCs within the dLN were analyzed for FITC-dextran uptake and expression of the influenza nucleocapsid (NP) protein. As shown in Fig. 4 a, a low but significant fraction (~15%) of LAPCs detected in the dLN of infected mice 24 h after FITC-dextran administration (i.e., 6 dpi) were FITC+NP+, consistent with the concept that the LAPCs had taken up viral antigen within the infected lungs and migrated to the dLNs over this 24-h time period. Both our previous (Yoo et al., 2010b) and current studies (Fig. 1 a and Fig. 4 a) suggest that significant LAPC migration out of the infected lungs and accumulation into the dLN starts between 5 and 6 dpi with IAV.

Based on late LAPC migration into the dLN, we reasoned that dLNs excised at 5 dpi, that is before LAPC migration out of the IAV-infected lungs, maintained ex vivo in culture for 24 h, would contain few if any LAPCs and not support Tfh differentiation. In contrast, inclusion of activated LAPCs to the dLN cultures would support Tfh differentiation (Fig. 4 b). Moreover, to further confirm the importance of ICOSL stimulation in LAPC-mediated Tfh differentiation, sorted 8 dpi LAPCs were pretreated with either isotype control Abs (Rat IgG) or αICOSL-blocking mAbs before i.v. transfer into mice. dLNs excised at 5 dpi and maintained in culture for 24 h before analysis contained few LAPCs and minimally supported Tfh differentiation compared with dLNs excised at 6 dpi and analyzed directly ex vivo (Fig. 4 c). In contrast, after i.v. transfer of LAPCs at 3 dpi and excision of the dLN at 5 dpi, both isotype

24 h after co-culture, Tfh differentiation (PD-1, CXCR5, and Bcl-6) and related cytokine production (IL-4 and IL-21) were examined in the TS-1 (Thy1.1+CD4+) population. Data are representative of at least two independent experiments are shown as means ± SEM Considered a significant difference at *, $P < 0.05$. (e) C57BL/6 mice ($n = 6$) were infected i.n. with a sublethal dose (0.05 LD50) of A/PR/8 virus. At 8 dpi, IL-4 production from Tfh cells (Thy1.2+CD4+PD-1+CXCR5+ or Thy1.2+CD4+CXCR5+Bcl-6+) was examined in the dLN by FACS analysis. The percentage of Tfh phenotypic cells, gated on IL-4+ CD4 T cells (Thy1.2+CD4+IL-4+), was also evaluated. Representative images from two independent experiments are shown.

control Ab–treated and αICOSL-blocking mAb treated LAPCs were readily detected in the excised dLN after 24 h culture. However, there was restoration of Tfh differentiation only in the dLNs isolated from the mice that received control Ab–treated LAPCs (Fig. 4 c). It is noteworthy that the frequencies of B cells and DCs, as well as cellular proliferation (determined by Ki-67$^+$ expression) were comparable between cultured dLN (Fig. 4 d, D5+1, ev) and in vivo isolated dLN (Fig. 4 d, D5+1, iv).

LAPC migration into the dLN is CXCR3 dependent

Our earlier reported gene expression profiling of LAPCs revealed that the gene encoding the chemokine receptor CXCR3 (rather than CCR7) was prominently expressed (Yoo et al., 2010b). In A/WSN/33 virus infection, LAPCs isolated from lung, but not dLN, expressed CXCR3 on their surface (Yoo et al., 2010b). We verified that after A/PR/8 infection CXCR3 was indeed expressed on the surface of LAPCs found in infected lungs (Fig. 5 a). This finding raised

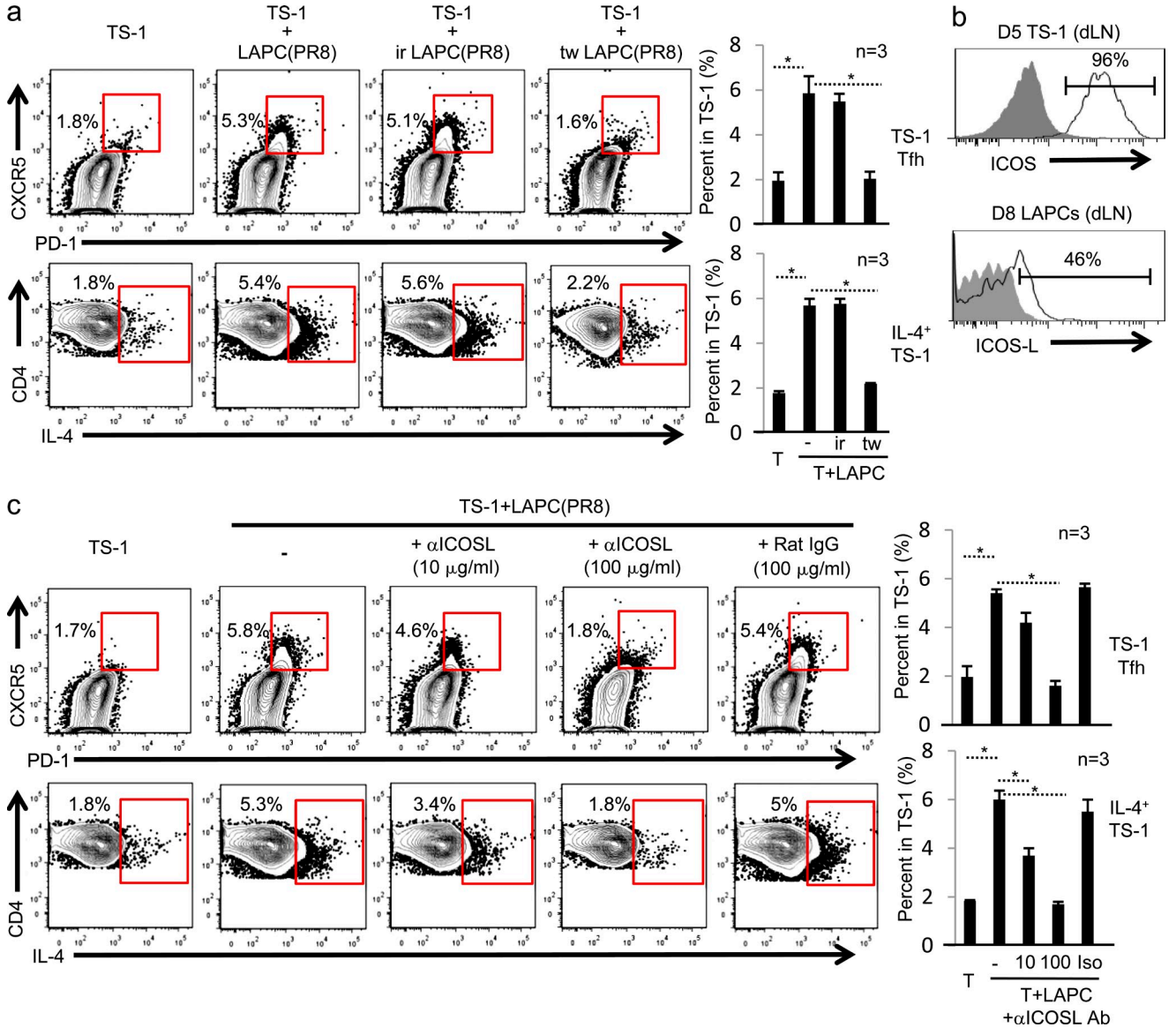

Figure 3. LAPCs promote IL-4$^+$ type-2 Tfh differentiation via ICOS–ICOSL–mediated interaction. (a) Sorted, in vivo Ag-primed 5 dpi TS-1 cells were incubated with either live or γ-irradiated (ir; 2,000 rads) 8 dpi LAPCs, which were isolated from the dLN of A/PR/8 virus–infected mice ($n = 8$). An aliquot of 5 dpi TS-1 cells were incubated with 8 dpi LAPCs, separated by a membrane (tw, transwell), according to the transwell protocol described in Materials and methods. Data are representative of at least two independent experiments are shown as means ± SEM. (b) ICOS and ICOSL expression were determined by FACS analysis on 5 dpi TS-1 T cells (Thy1.1$^+$CD4$^+$) and 8 dpi LAPCs (mPDCA1$^+$CD11c$^-$B220$^-$TcRβ$^-$), respectively. Data are representative of three independent experiments are shown. (c) To examine the molecular mechanisms involved in LAPC-mediated Tfh differentiation, 5 dpi TS-1 T cells were incubated with 8 dpi LAPCs, in the presence or absence of the indicated concentrations of ICOSL-blocking mAbs (HK5.3). At 24 h after incubation, the extent of Tfh differentiation (PD-1 and CXCR5) and related cytokine production (IL-4) were examined in the TS-1 (Thy1.1$^+$CD4$^+$) population. Data are representative of at least two independent experiments are shown as means ± SEM. *, $P < 0.05$.

the possibility that migration of LAPCs from infected lungs to the dLN might be regulated by a chemotactic stimulus mediated through CXCR3. Accordingly, we checked for expression of the cognate ligand for CXCR3, *Cxcl9*. Time course studies revealed that expression of *Cxcl9* is maximal in the dLN at 8 dpi, i.e., coincident with the time period of optimal LAPC migration to the dLN, and that LN-resident DCs and, to a lesser extent, macrophages were likely the primary sources of this chemokine in the lung dLN (Fig. 5 b).

To more directly assess the contribution of CXCR3 in the migration of LAPCs from infected lungs to the dLN, we next evaluated the migration of LAPCs after i.n. FITC-dextran administration and uptake by LAPCs in influenza-infected CXCR3-deficient and -sufficient (WT) mice. Although the absolute number of LAPCs in the infected lungs was not affected (not depicted), CXCR3 deficiency resulted in a marked decrease in accumulation of migratory LAPCs in the dLN at 6 dpi, also evident when LAPC accumulation was evaluated at 8 dpi (Fig. 5, c and d). Notable, CXCR3 deficiency did not have a substantial effect on the numbers of cells representative of other cell types present in either the infected lungs or dLN, when evaluated at 3 and 8 dpi (unpublished data).

The aforementioned results suggest that signaling through the CXCR3 may play a prominent role in the migration of

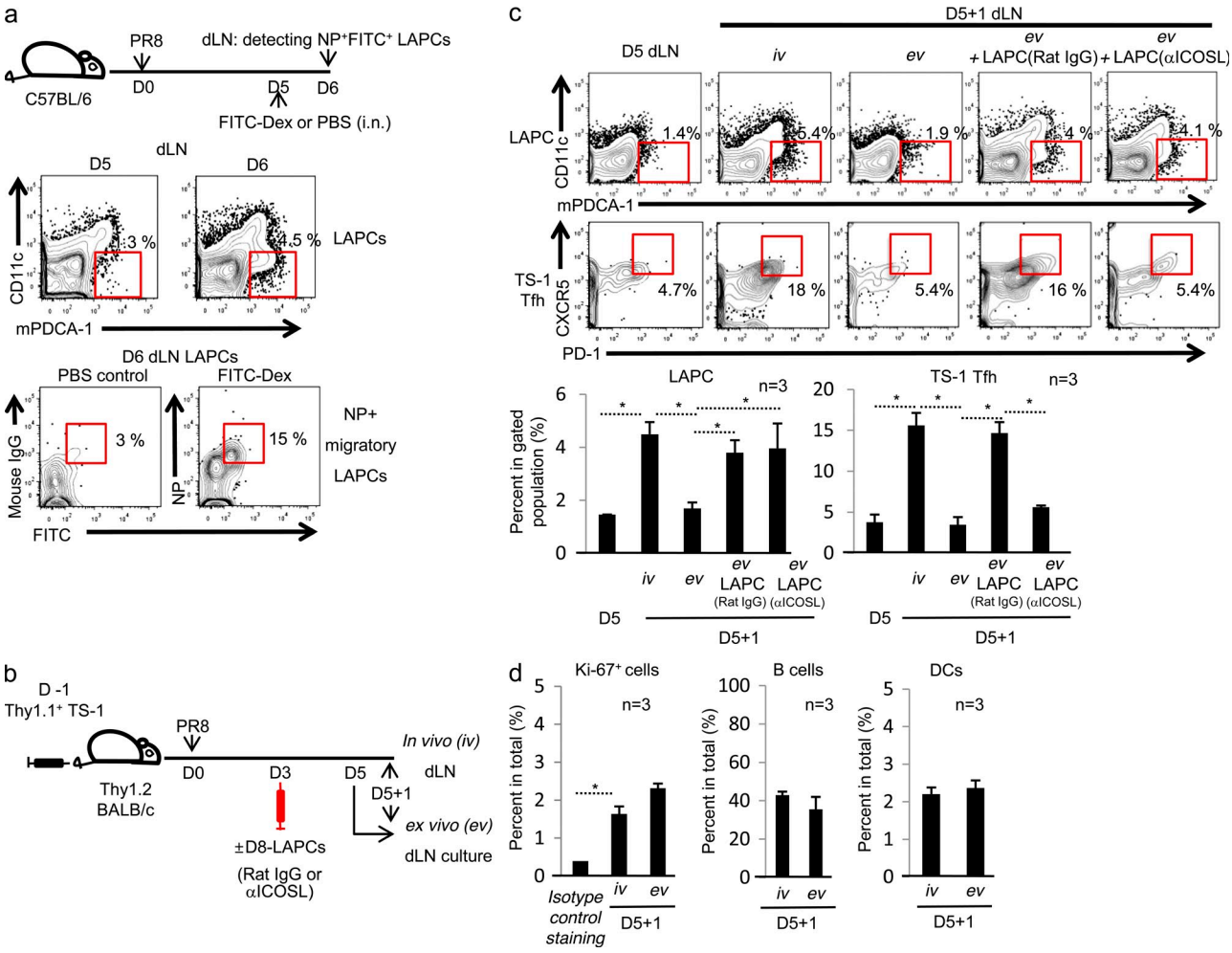

Figure 4. LAPCs modulate anti-IAV Tfh differentiation via ICOS stimulation in ex vivo LN organ culture. (a) To examine LAPC migration from lungs into dLN, an in vivo migration assay was performed as described in Materials and methods. LAPC (mPDCA1$^+$CD11c$^-$B220$^-$TcRβ$^-$) accumulation in the dLN was examined at 5 and 6 dpi by FACS analysis. 24 h after FITC-dextran treatment (6 dpi), cells were harvested from the dLNs (n = 12) and were stained for IAV-NP protein (intra-cellular). The percentage of FITC$^+$ NP$^+$ cells in the LAPC population was examined by FACS analysis. Representative images of two independent experiments are shown. (b–d) Thy1.1$^+$ TS-1 T cells were transferred into Thy1.2$^+$ WT mice as described in Materials and methods. The TS-1 T cell recipient mice (n = 30) were infected with A/PR/8 influenza 24 h later. At 3 dpi, groups of IAV-infected mice (n = 12) were inoculated i.v. with day 8 LAPCs (5×10^5 cells/mouse), isolated from the dLNs of A/PR/8 virus–infected BALB/c mice and pretreated with either rat IgG control Ab or αICOSL-blocking mAb (100 µg/ml). Intact dLNs (mediastinal LNs) from IAV-infected mice were excised on 5 dpi. The intact dLNs were cultured for 24 h in hyperoxy chambers, as described in Materials and methods, and then analyzed by FACS analysis for the presence of LAPCs (PDCA1$^+$CD11c$^-$B220$^-$TcRβ$^-$) and TS-1 Tfh cells (Thy1.1$^+$CD4$^+$PD-1$^+$CXCR5$^+$; c), and Ki-67$^+$ cells (Ki-67$^+$), B cells (B220$^+$TcRβ$^-$), and DCs (CD11c$^+$TcRβ$^-$; d). Data are representative of at least two independent experiments are shown as means ± SEM. *, $P < 0.05$.

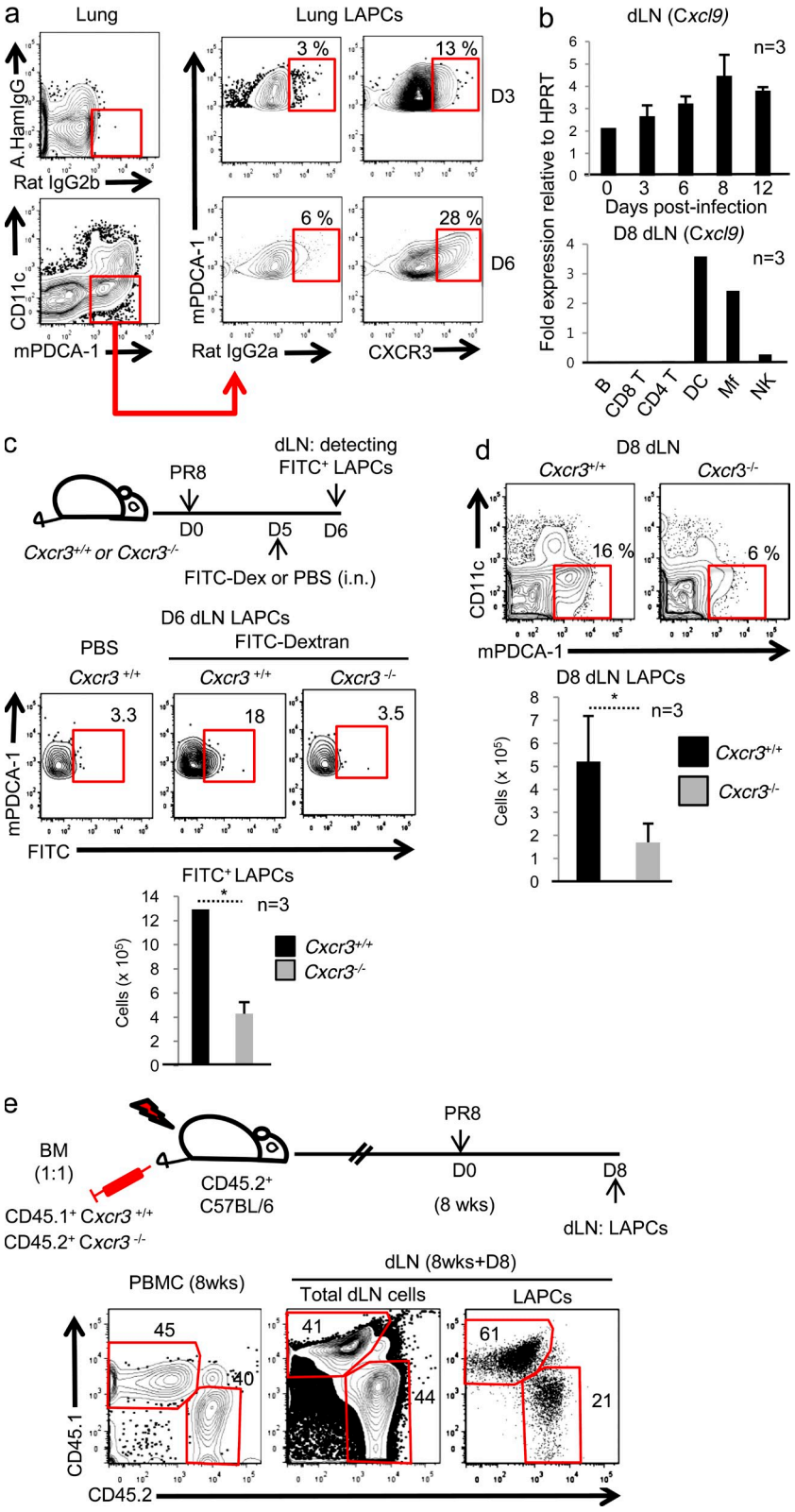

Figure 5. LAPC migration into the dLNs is CXCR3 dependent. (a) LAPCs (mPDCA1+CD11c−B220−TcRβ−) cell surface CXCR3 expression was examined by FACS analysis, using cells isolated from IAV-infected lungs (n = 12) on 3 and 6 dpi. Representative images of three independent experiments are shown. (b) At the indicated dpi, *Cxcl9* gene expression was determined by qPCR, either in total dLN cells (n = 24) or in each of the indicated cell populations isolated from the dLN of IAV-infected mice (n = 6). Representative data of two independent experiments are shown. To determine whether CXCR3–CXCL9 interactions are involved in LAPC migration into the dLN, an in vivo migration assay was performed using *Cxcr3*$^{-/-}$ mice. (c) Both WT (n = 9) and *Cxcr3*$^{-/-}$ mice (n = 9) were infected with IAV, and then FITC-dextran was administered i.n. on 5 dpi. 24 h later, cells were isolated from the dLNs and the extent of migratory LAPCs was determined by FACS analysis. Numbers indicate the percentage of FITC+ cells within the LAPC population. The absolute cell number of FITC+ LAPCs in the dLN was also determined and is shown as mean ± SEM. Representative data of two independent experiments are shown. (d) Both WT (n = 12) and *Cxcr3*$^{-/-}$ (n = 12) mice were infected with IAV. At 8 dpi the accumulation of LAPCs (mPDCA1+CD11c−B220−TcRβ−) in the dLN was examined by FACS analysis. Representative data of at least three independent experiments are shown. (e) Mixed BM chimera containing WT *and Cxcr3*$^{-/-}$ BM at a 1:1 ratio were generated as described in Materials and methods. At 8 wk after reconstitution, mice (n = 6) were infected with A/PR/8 virus. At 8 dpi, the ratio between WT and *Cxcr3*$^{-/-}$ LAPCs (mPDCA1+CD11c−B220−TcRβ−) was determined in the dLNs by FACS analysis. Representative images and data of at least two independent experiments are shown. *, $P < 0.05$.

LAPCs from infected lungs to the dLNs. To further address this possibility, we constructed mixed BM chimera consisting of lethally irradiated (1,100 rads) C57BL/6 mice reconstituted with a 1:1 mixture of BM from CD45 congenic CD45.1+*Cxcr3*$^{+/+}$ and CD45.2+ *Cxcr3* $^{-/-}$ mice. 8 wk after the successful BM reconstitution, mice were infected with A/PR/8 virus and 8 dpi the abundance of WT (CD45.1+) and *Cxcr3*$^{-/-}$ (CD45.2+) LAPCs in the dLN were determined (Fig. 5 e). Notably, although BM reconstitution of WT and *Cxcr3*$^{-/-}$ cells was comparable, as monitored by PBMC frequencies and total CD45+ cells in the dLN, at 8 dpi, WT LAPCs were three times more abundant than their *Cxcr3*$^{-/-}$ counterparts. The accumulation of other immune cell types (i.e., B/T lymphocytes and DCs) in the dLN after infection was not affected by CXCR3 deficiency (unpublished data). Collectively, these results suggest that the chemotactic stimulus provided by CXCR3–CXCL9 interactions is an important contributor, but not necessarily the sole contributor, to LAPC migration from infected lungs into the dLNs.

LAPCs promote Tfh differentiation and GC B cell responses during in vivo IAV infection

Given the evidence that LAPCs function as regulators of Tfh differentiation in the dLN after IAV infection, we evaluated the Tfh response and GC B cell generation at 8 dpi in WT and CXCR3-deficient mice, along with CXCR3-deficient mice that received either purified (FACS-sorted) WT LAPCs (mPDCA1$^+$CD11c$^-$B220$^-$TcRβ^-), DCs (CD11c$^+$TcRβ^-), or B cells (B220$^+$CD19$^+$CD11c$^-$) isolated from the dLNs at 8 dpi (Fig. 6 a). As depicted in Fig. 6 b, CXCR3-deficient mice exhibited a significant (~40%) reduction in both the frequency and absolute number of Tfh cells (Fig. 6 b) compared with infected WT mice. Concomitant with the diminished Tfh response, the generation of GC B cells was correspondingly reduced (Fig. 6 c). As noted in relation to Fig. 5, CXCR3 deficiency did not affect the total accumulation of CD4$^+$ T cells, B cells, and DCs in the dLNs of these mice at 8 dpi, which were comparable to that of infected WT mice (unpublished data). Moreover, B/T lymphocyte chimeric CXCR3 KO mice, which were reconstituted with WT B/T lymphocytes after depletion of recipient KO lymphocytes with depleting mAbs, showed comparable levels of Tfh accumulation in their dLN to that of nonchimeric CXCR3 KO mice at 8 dpi (unpublished data). Together, these data suggest that the defect in Tfh differentiation in IAV-infected CXCR3 KO mice may not be caused by the CXCR3 deficiency on other cell types, including lymphocytes and DCs. Of particular note, adoptive transfer of LAPCs into CXCR3-deficient infected mice not only reversed the deficit in Tfh T cells and GC B cells, but dramatically increased the numbers of these cells above the levels in the dLNs of infected WT mice (Fig. 6, b and c). Interestingly, adoptive transfer of B cells but not

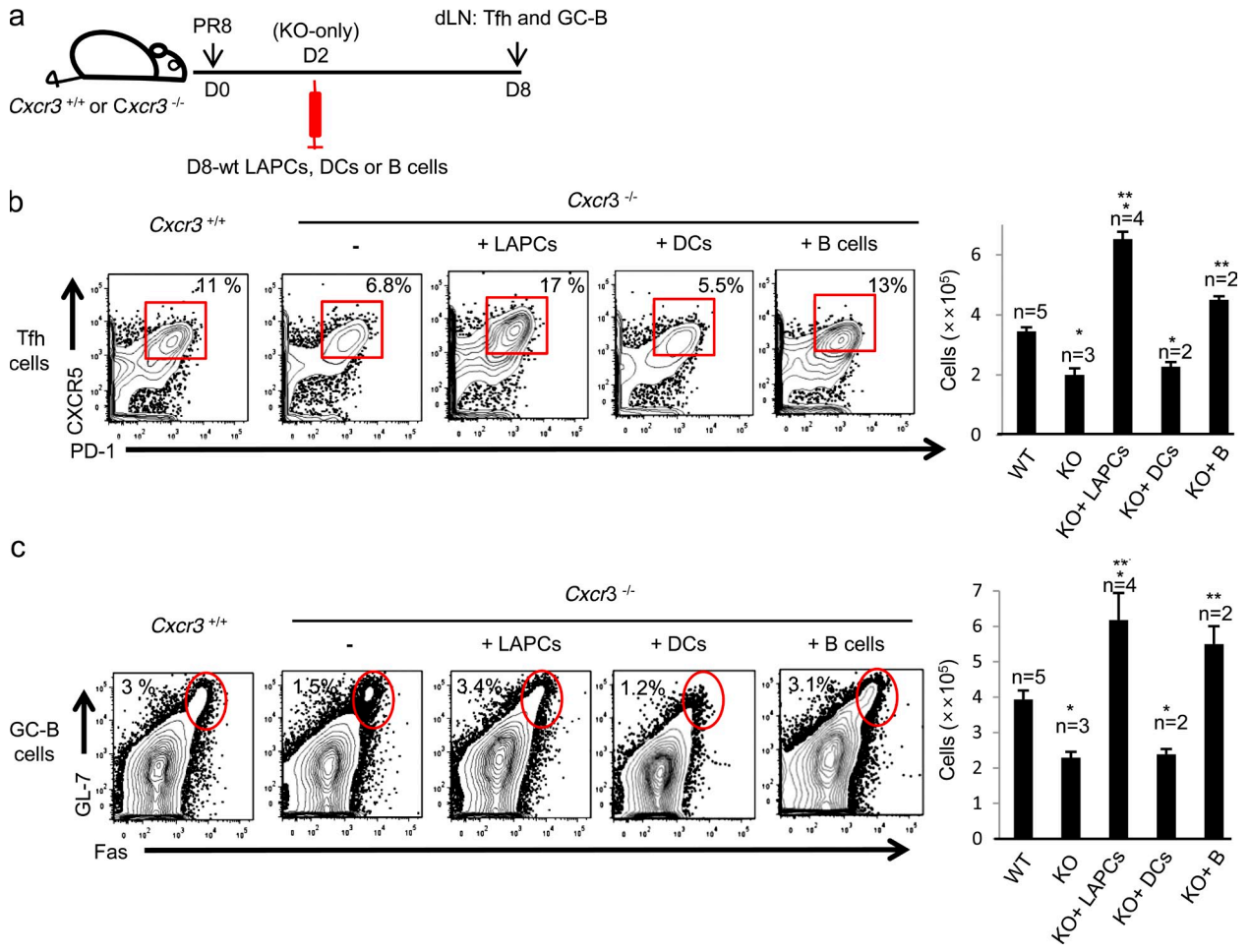

Figure 6. LAPCs promote both Tfh differentiation and GC B cell responses in IAV infection in vivo. (a) Both WT (n = 9) and *Cxcr3*$^{-/-}$ mice (n = 24) were infected with A/PR/8 virus. On 2 dpi, groups of IAV-infected *Cxcr3*$^{-/-}$ mice (n = 18) were inoculated i.v. with 8 dpi LAPCs (mPDCA1$^+$CD11c$^-$B220$^-$TcRβ^-), DCs (CD11c$^+$TcRβ^-), or B cells (B220$^+$CD19$^+$CD11c$^-$; 5 × 10^5 cells/mouse), isolated from the dLNs of different A/PR/8 virus–infected B6 mice. 8 dpi, both Tfh (PD-1$^+$CXCR5$^+$CD4$^+$Thy1.2$^+$; b) and GC B cells (B220$^+$Fas$^+$GL-7$^+$; c) responses were examined in the dLNs by FACS analysis and were compared between each group of mice. Representative images and data of three independent experiments are shown. The absolute cell numbers of Tfh and GC B cells in the dLN are also shown as mean ± SEM. Considered a significant difference at * (compared with WT) and ** (compared with *Cxcr3*$^{-/-}$, KO), $P < 0.05$.

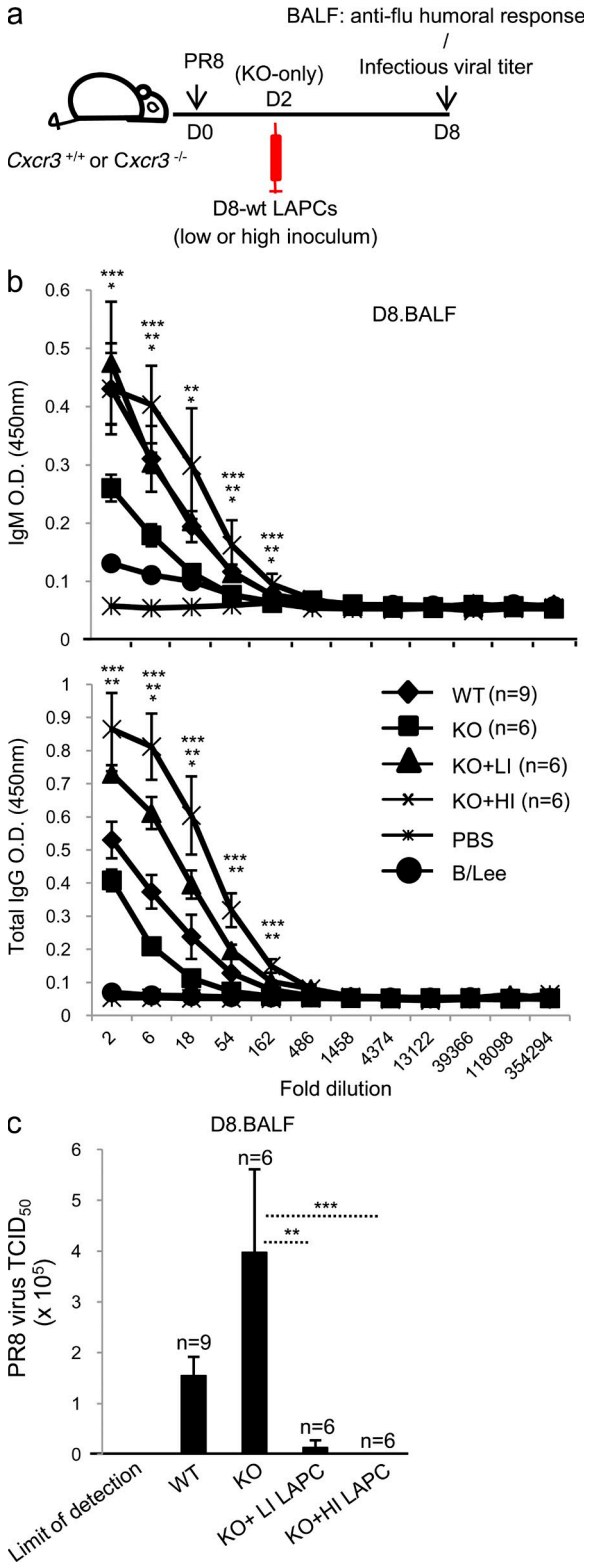

Figure 7. LAPCs control viral replication in the lung via modulating humoral responses in IAV infection. (a) Both WT ($n = 9$) and *Cxcr3*$^{-/-}$ mice ($n = 18$) were infected with A/PR/8 virus (0.05 LD50). At 2 dpi, groups of IAV-infected *Cxcr3*$^{-/-}$ mice ($n = 12$) received different inocula of 8 dpi LAPCs (mPDCA1^{+}CD11c^{-}B220^{-}TcRβ^{-}), (2.5×10^5 [LI] or 5×10^5 [HI] cells/mouse), i.v., isolated from the dLNs of different A/PR/8 virus-infected B6 mice. (b) Antiinfluenza Ab responses (IgM and total IgG) and (c) infectious viral titers were determined in the BAL fluid (BALF) by Ab-ELISA and $TCID_{50}$ assays, respectively, as described in Materials and methods. Combined data of two independent experiments are shown as means ± SEM. Considered a significant difference at * (KO vs. WT), ** (KO vs. KO+ LI LAPC) and *** (KO vs. KO + HI LAPC), $P < 0.05$.

DCs, harvested at 8 dpi from the dLNs, into infected CXCR3-deficient recipients also restores Tfh T cells and GC B cell responses in these mice to the levels observed in the WT mice.

Effects of LAPCs on the humoral immune response to IAV infection

Diminished LAPC migration out of infected lungs to the dLNs in CXCR3-deficient mice was associated with a diminished antiinfluenza Tfh response and reduced GC B cell numbers in the dLNs. Because the LNs draining the respiratory tract are believed to be the predominant site for the initiation of humoral responses during primary IAV infection (Waffarn and Baumgarth, 2011), we next examined whether alterations in LAPC homing (and associated alterations in Tfh and GC responses) had an impact on the humoral response in the lungs to IAV infection. We evaluated the antibody responses (by ELISA) at 8 dpi in the bronchoalveolar lavage (BAL) of CXCR3-deficient and WT mice during primary i.n. infection with A/PR/8 virus (Fig. 7 a). We found that *Cxcr3*$^{-/-}$ mice exhibited diminished IgM and IgG responses to A/PR/8 in their lungs compared with WT mice (Fig. 7 b). However, adoptive transfer of LAPCs restored the antiinfluenza humoral response in *Cxcr3*$^{-/-}$ mice. Indeed, CXCR3-deficient recipients of transferred LAPCs exhibited higher IgG antibody levels in their BAL compared with infected WT mice (Fig. 7 b). This augmentation of antibody responses by adoptively transferred LAPCs was dependent on the inoculating dose of LAPCs transferred. This was particularly evident in the case of IgG responses, where transfer of a larger number of LAPCs (HI, 5×10^5 cells/mouse) into *Cxcr3*$^{-/-}$ mice resulted in a greater increase in the IgG response than transfer of a lower number of LAPCs (LI, 2.5×10^5 cells/mouse).

Finally, we assessed the effect of diminished LAPC migration on virus clearance at 8 dpi in infected WT and CXCR3-deficient recipients. We found that CXCR3-deficient recipients had a modest but still significant elevation of pulmonary virus titer ($\approx 4 \times 10^5$) at 8 dpi compared with WT animals ($\approx 1.5 \times 10^5$; Fig. 7 c). Importantly, the transfer of LAPCs at 2 dpi resulted in dramatically enhanced infectious virus clearance from the BAL of CXCR3-deficient recipients, with recipients of the higher LAPC inoculum dose demonstrating more than a three log-fold reduction in pulmonary virus titer ($\approx 1 \times 10^2$) compared with untreated CXCR3-deficient animals ($\approx 4 \times 10^5$).

DISCUSSION

Because they were first identified in human tonsils (Breitfeld et al., 2000; Schaerli et al., 2000; Kim et al., 2001), Tfh T cells (defined as PD-1$^+$CXCR5$^+$Bcl-6$^+$ CD4$^+$ T cells) have been implicated as key regulators of the GC B cell response, which in turn is important in pathogen clearance and is essential in preventing repeat infections with many pathogens (Graham and Braciale, 1997; Baumgarth et al., 2000; Vinuesa et al., 2005; King et al., 2008, Crotty, 2011; Waffarn and Baumgarth, 2011). GC B cell responses include BcR affinity maturation and memory B cell formation (Crotty, 2011). Tfhs control the GC B cell response via multiple molecular mechanisms, including cytokine production (IL-4 and IL-21) and the delivery of co-stimulatory signals (CD40L). The process of Tfh differentiation and its control are not fully understood and multiple mechanisms have been invoked to explain these processes (Crotty, 2011).

Initially, it was suggested that soluble factors, including IL-6 and/or IL-21, are sufficient to drive Tfh differentiation from naive CD4$^+$ T cells both in vitro and in vivo (Nurieva et al., 2008, 2009). It is unclear whether these soluble factors can directly induce Tfh differentiation from naive CD4$^+$ T cells because in some studies these findings were not recapitulated (Dienz et al., 2009; Eto et al., 2011). Nonetheless, as previously reported (Nurieva et al., 2008; Vogelzang et al., 2008; Eto et al., 2011), we do find that IAV-infected IL-21R$\alpha^{-/-}$ mice displayed a substantially reduced overall Tfh response in the dLN (unpublished data), suggesting that IL-21 may play a role in modulating the induction or maintenance of the Tfh response during pulmonary IAV infection.

Based largely on observations using B cell–deficient mice (μMT), it has been suggested that B cells are key regulators of Tfh differentiation (Haynes et al., 2007; Johnston et al., 2009; Zaretsky et al., 2009). Although these results would strongly argue for a role of B cells in the induction of the Tfh response, surprisingly, in our hands neither total B cells (B220$^+$CD19$^+$CD11c$^-$) nor activated B cells (B220$^+$ CD19$^+$CD69$^+$CD11c$^-$) isolated from the dLN of IAV-infected mice efficiently induce Tfh differentiation by Ag-primed CD4$^+$ T cells (Fig. 2 b). A similar inability of in vivo–isolated, Ag-presenting activated B cells to induce Tfh differentiation from naive CD4$^+$ T cells in vitro, in co-culture experiments, has been reported (Pelletier et al., 2010). However, we have observed that similar to LAPC adoptive transfer, the adoptive transfer of IAV-activated B cells also results in an increase in Tfh cells in the dLN (Fig. 6 b), despite their inability to drive Tfh differentiation in vitro. The enhanced Tfh response after transfer of IAV-activated B cells may reflect the ability of B cells to sustain a developing Tfh response, but could also reflect the capacity of B cells generated during respiratory virus infection to also drive Tfh differentiation in the environment of the inflamed dLN.

After systemic infection with LCMV, Tfh differentiation is observed early after infection, i.e., ~2 dpi, presumably during the initial phase of CD4$^+$ T cell induction by DCs (Choi et al., 2011). Adoptive transfer of in vitro–activated splenic DCs pulsed with a high concentration of antigen into naive mice also induces Tfh differentiation in vivo. In this model, as supported by other studies (Baumjohann et al., 2011; Kerfoot et al., 2011; Kitano et al., 2011), the differentiation of antigen-activated CD4$^+$ T cells into Bcl-6$^+$CXCR5$^+$ Tfh cells (rather than Blimp1$^+$T-bet$^+$ TH1 effector T cells) occurred early after initial cell division and was dependent on IL-2Rα (CD25) expression. However, in the ex vivo co-culture analysis of Tfh differentiation used here, we found that DCs isolated from the dLN of IAV-infected mice 3 dpi could induce T-bet$^+$ TH1 but not Bcl-6$^+$ Tfh differentiation from naive CD4$^+$ T cells (unpublished data). It is also noteworthy that CD4$^+$ T cells isolated from the dLN of IAV-infected mice 5 dpi, which had completed up to 8 or 9 rounds of cell division, did not yet display the Tfh phenotype (Fig. 1 c). Co-culture of these antigen-activated CD4$^+$ T cells with activated DCs isolated from the dLN of the IAV-infected mice on 8 dpi triggered only a modest increase in Tfh cell numbers ex vivo (Fig. 2 b). In addition, adoptive transfer of in vivo IAV-activated dLN DCs into IAV-infected recipients did not enhance Tfh accumulation in the recipient mice (Fig. 6 b). These data suggest that the process of Tfh differentiation and the cell types regulating this process may differ between systemic viral infections e.g., LCMV and viral infections initiated at mucosal surfaces, such as a IAV infection in the lungs.

In pulmonary IAV infection, the kinetics of Tfh T cell generation/accumulation are slower than that reported for systemic infection in the LCMV model (Choi et al., 2011); we could detect Tfh cells in the dLN from 6 dpi (Fig. 1). These kinetic differences most likely represent differences caused by the inoculating virus dose, the route of infection, and the rate of virus replication. The kinetics of Tfh accumulation in the dLNs correlated with LAPC migration into the dLNs (Fig. 1). Both our ex vivo and in vivo analyses suggest that in pulmonary IAV infection, LAPCs promote Tfh differentiation of Ag-primed CD4$^+$ T cells (Figs. 2, 4, and 6). In this regard, it is noteworthy that the induction of potent humoral responses to IAV in the mouse model is reported to be dependent not on the presence of CD11c$^+$ cells, but rather on the response of mPDCA-1$^+$ cells (GeurtsvanKessel et al., 2008). Although the authors reported that mPDCA-1$^+$CD11c^{lo} pDCs were implicated in the control of the humoral response to IAV infection, LAPCs are also mPDCA-1$^+$ (and CD11c$^-$), making LAPCs an attractive alternative mPDCA-1$^+$ candidate regulator of Tfh-dependent antibody production. Moreover, we have observed that IL-21R$\alpha^{-/-}$ mice, which exhibit a defective Tfh response (Nurieva et al., 2008; Vogelzang et al., 2008; Eto et al., 2011), also exhibit significantly impaired migration of LAPCs from the IAV-infected lungs into the dLNs, compared with WT mice (unpublished data). The underlying mechanisms linking impaired LAPC migration and a defective Tfh response to IL-21R signaling are the subject of our ongoing investigations.

LAPCs have previously been shown to stimulate IAV-specific TH2 effector T cell (GATA-3$^+$IL-4$^+$) differentiation (Yoo et al., 2010a,b). More than 75% of IL-4$^+$ CD4$^+$ T cells

in the dLNs of IAV-infected mice on 8 dpi also exhibited the characteristic phenotype of Tfh cells (PD-1$^+$CXCR5$^+$; Fig. 2 e). This result was not unexpected, as the majority of IL-4–producing CD4$^+$ T cells in the dLNs responding to helminth infection also display a Tfh phenotype (PD-1$^+$ CXCR5$^+$ Bcl-6$^+$IL-21$^+$; King and Mohrs, 2009; Zaretsky et al., 2009), findings that are consistent with the view that TH2 and Tfh effector T cells may be phenotypically similar, if not overlapping T cell subsets. We also found that although the encounter of activated, IAV-specific CD4$^+$ T cells with LAPCs resulting in Tfh cell differentiation did not require recognition of specific antigen by the activated CD4$^+$ T cells, efficient production of IL-4 by the Tfh cells required antigen-specific (cognate) interactions between the activated CD4$^+$ T cells and LAPCs (Fig. 2, b and c). The significance of this differential requirement for specific antigen display by LAPC to stimulate the expression of phenotypic markers characteristic of Tfh differentiation and the capacity of Tfh cells to produce IL-4, is not yet clear. However, IL-4 is a critical cytokine produced by Tfh cells, required to support GC B cell responses (Yusuf et al., 2010; Crotty, 2011). Perhaps, cognate antigen recognition by the differentiating Tfh cells i.e., engagement of the TcR, is essential to complete the formation of fully functional Tfh cells capable of optimal effector functions relevant for B cell responses.

We found that cell-cell contact was crucial for LAPC-mediated type-2 Tfh differentiation (Fig. 3 a). This finding in part reflects the need for ICOS–ICOSL interactions between the T cells and the LAPCs, as blockade of this interaction in both ex vivo LAPC-T cell co-cultures and ex vivo dLN cultures by blocking antibodies markedly diminished the differentiation of activated CD4$^+$ T cells into Tfh cells (Fig. 3, b and c, and Fig. 4 c). It is noteworthy that both DCs and B cells in the IAV dLNs express levels of ICOSL on their surface that are comparable to levels expressed by LAPCs (unpublished data). However, these cells could not induce Tfh differentiation as efficiently as LAPCs (Fig. 2 b). Therefore, even though ICOS–ICOSL interactions are necessary for Tfh differentiation, one or more additional factors, presumably cell surface molecules, contribute to the enhanced ability of LAPCs to support Tfh differentiation. We have examined the role of PDL1, which is expressed by IAV activated LAPCs (PDL2 expression was not detected on LAPC), in regulating LAPC-mediated Tfh differentiation ex vivo by blocking Ab treatment (10F.9G2). However, we find that blockade of PD-1–PDL1 interactions in LAPC-T cell co-cultures has no effect on LAPC-mediated Tfh differentiation (unpublished data).

We demonstrated that IAV-infected *Cxcr3*$^{-/-}$ mice exhibit diminished LAPC migration into the dLNs (Fig. 5), implicating this chemokine receptor in regulation of the LAPC migration from the infected lungs into the dLN. Reduced LAPC migration was associated with a corresponding diminished Tfh response and reduced antiinfluenza humoral responses (Fig. 6). The reduced A/PR/8 virus-specific humoral (IgM and IgG) response associated with diminished LAPC migration directly affected infectious viral titers in the lungs of A/PR/8 virus-infected mice (Fig. 7, b and c). Adoptive transfer of A/PR/8 virus infection–sensitized dLN LAPCs into A/PR/8 virus–infected *Cxcr3*$^{-/-}$ recipient mice enhanced the humoral antibody response and augmented IAV clearance from infected lungs. However, the effects of an enhanced humoral response on viral clearance in IAV-infected mice can vary based on viral strains and the genetic background of the mice (Topham et al., 1996; Brown et al., 2006; GeurtsvanKessel et al., 2008; Sundararajan et al., 2012). As shown here (Fig. 7), generally in A/PR/8 virus infection the host humoral response is crucial to control viral replication: viral titers in the lungs show an inverse correlation with the extent of the host humoral response (Brown et al., 2006). However, in some other IAV strains, the host humoral response does not seem to be crucial for viral clearance (Topham et al., 1996; GeurtsvanKessel et al., 2008). Certainly, in our previous studies using A/WSN/33 virus and WT B6 mice, even though LAPC adoptive transfer augmented the host humoral response, this did not lead to accelerated viral clearance in the lungs of recipient mice (Yoo et al., 2010b). Rather, LAPC transfer induced slightly delayed viral clearance in the recipient mice (twofold increase in viral titer) with enhanced type 2 immunity in the lungs of recipient mice, which correlates with our earlier observation that in A/JAPAN/57-infected mice, enhanced type 2 immunity can lead to delayed viral clearance in the lungs (Graham et al., 1994). Recently, Sundararajan et al. (2012) have suggested that, in IAV infection, the differences in viral strains and the genetic backgrounds of the mice lead to different outcomes in host immune responses, which ultimately can lead to different outcomes in viral clearance. Therefore, it is not altogether unexpected that in our studies using different viral strains (A/PR/8 vs. A/WSN/33) and genetic backgrounds (WT vs. CXCR3 KO) we observe different outcomes.

In conclusion, the findings in this paper suggest that a novel APC type, LAPC, which migrates from the virus-infected respiratory tract to the dLN, may play a critical role in regulating the differentiation of Ag-primed CD4$^+$ T cells into Tfh cells. Because of the late migration of LAPCs from the infected respiratory tract to the site of CD4$^+$ T cell activation and differentiation, LAPCs may be uniquely positioned to monitor the extent of microbial replication in the respiratory tract after the initial induction of T cell responses by DCs in the dLN and thereby regulate the balance between tissue migrating TH1 effector CD4$^+$ T cell and antibody-supporting CD4$^+$ Tfh differentiation.

MATERIALS AND METHODS

Mice and infections. C57BL/6 and BALB/c mice were purchased from Taconic or The Jackson Laboratory. *Cxcr3*$^{-/-}$ mice were provided by D. Mullins (University of Virginia, Charlottesville, VA) and CD45.1$^+$ mice were provided by K. Tung (University of Virginia, Charlottesville, VA). TS-1 mice were bred in house. All mice were housed in a specific pathogen–free environment and all mouse experiments were performed in accordance with protocols approved by the University of Virginia Animal Care and Use Committee. For virus infection, mice were infected i.n. with a sublethal dose (0.05 LD_{50}) of influenza strain A/PR/8/34 or X31 in serum-free Iscove's medium, after anesthesia with ketamine and xylazine.

Quantitative RT-PCR. dLN cell suspensions were prepared as previously described (Yoo et al., 2010a,b). Specific cell types were isolated by FACS (Reflection HAPS 2) to examine *Cxcl9* expression. mRNA isolation, reverse transcription, and real-time PCR were performed as previously described (Sun et al., 2009). Data were generated with the comparative threshold cycle method, by normalizing to hypoxanthine phosphoribosyltransferase (*Hprt*). The sequences of primers used in the studies are available on request.

BM chimeras. To generate mixed BM chimeras containing WT and *Cxcr3*$^{-/-}$ BM in a 1:1 ratio, we lethally irradiated (1,100 rads) CD45.2$^+$ WT mice and reconstituted the irradiated mice with CD45.1$^+$ WT BM (2×10^6 cells) mixed with CD45.2$^+$ *Cxcr3*$^{-/-}$ BM (2×10^6 cells). After 8 wk, the reconstitution efficiency was determined by FACS analysis, and the successfully reconstituted mice (reconstituted almost for 1:1 ratio in periphery) were then infected with A/PR/8 IAV.

TS-1 T cell transfer and infection. For TS-1 T cell transfer into Thy1.2$^+$ WT mice, cells were isolated from Thy-1.1$^+$ TS-1 LNs. A total of 5×10^6 LN cells were then transferred into Thy-1.2$^+$ mice by i.v. injection. The recipient mice were infected with A/PR/8 influenza 24 h later. At 5 dpi, in vivo virus–activated TS-1 cells were isolated by FACS and used for ex vivo co-culture experiments.

Cell sorting. For ex vivo co-culture experiments and adoptive transfer experiments, recipients of transferred TS-1 T cells or control, WT mice were infected with A/PR/8 influenza. Different cell populations from the dLN were sorted by FACS (Reflection HAPS 2) based on the following markers at either 5 or 8 dpi: TS-1 cells, Thy1.1$^+$CD4$^+$; B cells, B220$^+$CD19$^+$CD11c$^-$; activated B cells, B220$^+$CD19$^+$CD69$^+$CD11c$^-$; DCs, CD11c$^+$TcRβ^-; LAPCs, mPDCA1$^+$CD11c$^-$B220$^-$TcRβ^-. For *Cxcl9* qPCR, each indicated cell population was sorted from the dLN of IAV-infected WT mice based on the following markers at either 6 or 8 dpi: CD4 T cells, Thy1.2$^+$CD4$^+$; CD8 T cells, Thy1.2$^+$CD8α^+; B cells, B220$^+$CD19$^+$; NK cells, NK1.1$^+$Thy1.2$^-$; DCs, CD11c$^+$Thy1.2$^-$; Mϕ, F4.80$^+$.

Antibodies and FACS analysis. All antibodies were purchased from BD or eBioscience (unless otherwise stated): CD4 (L3T4), CD8α (53–6.7), CD11b (M1/70), CD11c (HL3), CD45.1 (A20), CD45.2 (104), CD90.1 (HIS51), CD90.2 (30-H12), CD19 (MB19-1), B220/CD45R (RA3-6B2), CD69 (H1.2F3), NK1.1 (PK136), F4/80 (BM8), TCRβ (H57-597), IL-4 (11B11), IL-21 (FFA21), Bcl6 (GI191E), CXCR5 (2G8), PD-1 (RMP1-30), ICOS (7E.17G9), ICOSL (HK5.3), Fas (Jo2), and GL-7 (GL7). A FITC-conjugated mAb to mPDCA-1 (JF05-1C2.4.1) was purchased from Miltenyi Biotec. A CXCR3-specific mAb was obtained from both R&D Systems (220803) and BioLegend (CXCR3-173). Flow cytometry was performed on FACS-Canto with optimal compensation set for six-color staining. The data were analyzed using FlowJo software (Tree Star).

In vivo migration assay. Mice were anesthetized as described above and infected by i.n. instillation with 50 µl PBS containing 0.05 LD_{50} A/PR/8 IAV. At 5 dpi, mice received 50 µl of either PBS (negative control) or FITC-dextran (40 kD, 1 mg/ml) by i.n. instillation. At 24 or 72 h after treatment, mice were sacrificed and cells were collected from the dLN. FACS analysis was performed to examine the percent population of FITC$^+$ cells gating on LAPCs (mPDCA-1$^+$CD11c$^-$B220$^-$TCRβ^-).

Transwell cultures. To examine whether soluble factors are critical for LAPC-mediated Tfh differentiation, transwell experiments were performed. In brief, FACS-sorted day 5 TS-1 cells were added into the lower chamber of a 96-well transwell plate (5×10^4 cells/well) and FACS-sorted 8 dpi LAPCs were introduced into the upper chamber (2.5×10^4 cells/well), which was separated with a 0.4-µm pore membrane (Costar; Corning). All experiments were performed in duplicate. After 24 h, TS-1 cells in the lower chamber were harvested, stained for IL-4, CXCR5, and PD-1 expression, and then examined by FACS analysis.

Adoptive transfer of IAV–activated LAPCs. Mice were infected with 0.05 LD_{50} of A/PR/8 virus. On 8 dpi, mice were sacrificed and IAV–activated LAPCs were harvested from the dLNs by FACS. Sorted LAPCs in 200 µl of sterile PBS (or PBS buffer alone) were injected into A/PR/8 virus–infected (0.05 LD_{50}) *Cxcr3*$^{-/-}$ mice on 2 dpi (low inoculum LAPC: 2.5×10^5 cells/mouse; high inoculum LAPC: 5×10^5 cells/mouse) by the i.v. route.

IAV–specific antibody ELISA. BAL fluid was collected from IAV–infected mice on 8 dpi by intratracheal instillation of 500 µl of sterile PBS, and antiinfluenza antibody responses in the BAL fluid were measured by ELISA. In brief, 96-well plates were coated overnight at room temperature with 50 µl of either A/PR/8 or B/Lee influenza virus. The plates were washed twice with PBS supplemented with 0.05% Tween-20 (PBST) and incubated with 50 µl of 2% BSA in PBST for 1 h at room temperature. After washing the plates with PBST, 50 µl of diluted BAL fluid was added to each well and incubated for 2 h at room temperature. Bound antibodies were detected by the incubation of horseradish peroxidase–conjugated anti–mouse IgM (1:10,000; SouthernBiotech) or total IgG (1:10,000; SouthernBiotech) antibodies. After 1 h, the plates were washed with PBST, and 100 µl of 3,3′,5,5′-tetramethylbenzidine (TMB) substrate solution (Sigma-Aldrich) was added into each well and incubated for an additional 30 min. The enzyme reaction was stopped by adding 100 µl of 2N H_2SO_4 and OD values were determined at 450 nm using a plate reader (Bio-TEK).

Virus titration. We monitored lung viral titers via endpoint dilution assay and expressed titers as a 50% tissue culture infective dose ($TCID_{50}$). In brief, Madin-Darby canine kidney cells (American Type Culture Collection) were seeded in individual wells of 96-well tissue culture plates and the resultant monolayers of cells were infected with 10-fold serial dilutions of BAL fluid from IAV–infected mice in 2% trypsin supplemented serum-free IMDM media. After 4 d of incubation, culture medium was harvested and mixed with an equal volume of 1% chicken RBCs (University of Virginia Veterinary Facilities). Hemagglutination patterns were recorded, and $TCID_{50}$ values calculated.

Ex vivo LN organ culture. Thy1.1$^+$ TS-1 T cells were transferred into Thy1.2$^+$ WT mice by i.v. inoculation into the tail vein. The TS-1 recipient mice were infected i.n. with a sublethal dose of IAV (A/PR/8, 0.05 LD_{50}) 24 h later. On 3 dpi, groups of mice received i.v. inoculation with either isotype control (Rat IgG) Ab-pretreated or αICOSL-blocking mAb-pretreated (100 µg/ml) activated LAPCs (5×10^5 cells/mouse; excess Abs were removed by washing with PBS twice before LAPC transfer). Intact dLNs from IAV-infected mice were excised at 5 dpi. The intact dLNs were placed in complete DMEM media, cultured under hyperoxic conditions (modular incubator chamber filled with 100% oxygen; Billups-Rothenberg) for 24 h, and then analyzed for the presence of LAPCs and Tfh cells by FACS analysis.

Statistical analysis. Unless otherwise noted, an unpaired two-tailed Student's *t* test was used to compare two treatment groups. Groups larger than two were analyzed with one-way ANOVA (Tukey's post-test). These statistical analyses were performed using Prism3 software (for Macintosh; GraphPad Software, Inc.). Data are mean ± SEM. A P value of < 0.05 was considered to be statistically significant.

We thank the members of Dr. Braciale's laboratory for critical comments and B. Small for excellent technical assistance. We thank D. Mullins and K. Tung for reagents.

This work was supported by United States Public Health Service grants AI-15608, HL-33391, AI-37293, and U19 AI-083024 to T.J. Braciale.

The authors declare no competing financial interests.

J.K. Yoo performed the experimental work and T.J. Braciale supervised the project. The manuscript was written by J.K. Yoo, E.N. Fish, and T.J. B. All authors approved the final manuscript.

Submitted: 24 October 2011
Accepted: 15 August 2012

REFERENCES

Baumgarth, N., O.C. Herman, G.C. Jager, L.E. Brown, L.A. Herzenberg, and J. Chen. 2000. B-1 and B-2 cell-derived immunoglobulin M antibodies are nonredundant components of the protective response to influenza virus infection. *J. Exp. Med.* 192:271–280. http://dx.doi.org/10.1084/jem.192.2.271

Baumjohann, D., T. Okada, and K.M. Ansel. 2011. Cutting Edge: Distinct waves of BCL6 expression during T follicular helper cell development. *J. Immunol.* 187:2089–2092. http://dx.doi.org/10.4049/jimmunol.1101393

Breitfeld, D., L. Ohl, E. Kremmer, J. Ellwart, F. Sallusto, M. Lipp, and R. Förster. 2000. Follicular B helper T cells express CXC chemokine receptor 5, localize to B cell follicles, and support immunoglobulin production. *J. Exp. Med.* 192:1545–1552. http://dx.doi.org/10.1084/jem.192.11.1545

Brown, D.M., A.M. Dilzer, D.L. Meents, and S.L. Swain. 2006. CD4 T cell-mediated protection from lethal influenza: perforin and antibody-mediated mechanisms give a one-two punch. *J. Immunol.* 177:2888–2898.

Choi, Y.S., R. Kageyama, D. Eto, T.C. Escobar, R.J. Johnston, L. Monticelli, C. Lao, and S. Crotty. 2011. ICOS receptor instructs T follicular helper cell versus effector cell differentiation via induction of the transcriptional repressor Bcl6. *Immunity*. 34:932–946. http://dx.doi.org/10.1016/j.immuni.2011.03.023

Crotty, S. 2011. Follicular helper CD4 T cells (TFH). *Annu. Rev. Immunol.* 29:621–663. http://dx.doi.org/10.1146/annurev-immunol-031210-101400

Dienz, O., S.M. Eaton, J.P. Bond, W. Neveu, D. Moquin, R. Noubade, E.M. Briso, C. Charland, W.J. Leonard, G. Ciliberto, et al. 2009. The induction of antibody production by IL-6 is indirectly mediated by IL-21 produced by CD4+ T cells. *J. Exp. Med.* 206:69–78. http://dx.doi.org/10.1084/jem.20081571

Eto, D., C. Lao, D. DiToro, B. Barnett, T.C. Escobar, R. Kageyama, I. Yusuf, and S. Crotty. 2011. IL-21 and IL-6 are critical for different aspects of B cell immunity and redundantly induce optimal follicular helper CD4 T cell (Tfh) differentiation. *PLoS ONE.* 6:e17739. http://dx.doi.org/10.1371/journal.pone.0017739

GeurtsvanKessel, C.H., M.A. Willart, L.S. van Rijt, F. Muskens, M. Kool, C. Baas, K. Thielemans, C. Bennett, B.E. Clausen, H.C. Hoogsteden, et al. 2008. Clearance of influenza virus from the lung depends on migratory langerin+CD11b- but not plasmacytoid dendritic cells. *J. Exp. Med.* 205:1621–1634. http://dx.doi.org/10.1084/jem.20071365

Graham, M.B., and T.J. Braciale. 1997. Resistance to and recovery from lethal influenza virus infection in B lymphocyte-deficient mice. *J. Exp. Med.* 186:2063–2068. http://dx.doi.org/10.1084/jem.186.12.2063

Graham, M.B., V.L. Braciale, and T.J. Braciale. 1994. Influenza virus-specific CD4+ T helper type 2 T lymphocytes do not promote recovery from experimental virus infection. *J. Exp. Med.* 180:1273–1282. http://dx.doi.org/10.1084/jem.180.4.1273

Haynes, N.M., C.D. Allen, R. Lesley, K.M. Ansel, N. Killeen, and J.G. Cyster. 2007. Role of CXCR5 and CCR7 in follicular Th cell positioning and appearance of a programmed cell death gene-1high germinal center-associated subpopulation. *J. Immunol.* 179:5099–5108.

Johnston, R.J., A.C. Poholek, D. DiToro, I. Yusuf, D. Eto, B. Barnett, A.L. Dent, J. Craft, and S. Crotty. 2009. Bcl6 and Blimp-1 are reciprocal and antagonistic regulators of T follicular helper cell differentiation. *Science.* 325:1006–1010. http://dx.doi.org/10.1126/science.1175870

Kadkhoda, K., S. Wang, Y. Fan, H. Qiu, S. Basu, A.J. Halayko, and X. Yang. 2011. ICOS ligand expression is essential for allergic airway hyperresponsiveness. *Int. Immunol.* 23:239–249. http://dx.doi.org/10.1093/intimm/dxq476

Kerfoot, S.M., G. Yaari, J.R. Patel, K.L. Johnson, D.G. Gonzalez, S.H. Kleinstein, and A.M. Haberman. 2011. Germinal center B cell and T follicular helper cell development initiates in the interfollicular zone. *Immunity.* 34:947–960. http://dx.doi.org/10.1016/j.immuni.2011.03.024

Kim, T.S., and T.J. Braciale. 2009. Respiratory dendritic cell subsets differ in their capacity to support the induction of virus-specific cytotoxic CD8+ T cell responses. *PLoS ONE.* 4:e4204. http://dx.doi.org/10.1371/journal.pone.0004204

Kim, C.H., L.S. Rott, I. Clark-Lewis, D.J. Campbell, L. Wu, and E.C. Butcher. 2001. Subspecialization of CXCR5+ T cells: B helper activity is focused in a germinal center-localized subset of CXCR5+ T cells. *J. Exp. Med.* 193:1373–1381. http://dx.doi.org/10.1084/jem.193.12.1373

King, I.L., and M. Mohrs. 2009. IL-4-producing CD4+ T cells in reactive lymph nodes during helminth infection are T follicular helper cells. *J. Exp. Med.* 206:1001–1007. http://dx.doi.org/10.1084/jem.20090313

King, C., S.G. Tangye, and C.R. Mackay. 2008. T follicular helper (TFH) cells in normal and dysregulated immune responses. *Annu. Rev. Immunol.* 26:741–766. http://dx.doi.org/10.1146/annurev.immunol.26.021607.090344

Kitano, M., S. Moriyama, Y. Ando, M. Hikida, Y. Mori, T. Kurosaki, and T. Okada. 2011. Bcl6 protein expression shapes pre-germinal center B cell dynamics and follicular helper T cell heterogeneity. *Immunity.* 34:961–972. http://dx.doi.org/10.1016/j.immuni.2011.03.025

Lee, S.K., R.J. Rigby, D. Zotos, L.M. Tsai, S. Kawamoto, J.L. Marshall, R.R. Ramiscal, T.D. Chan, D. Gatto, R. Brink, et al. 2011. B cell priming for extrafollicular antibody responses requires Bcl-6 expression by T cells. *J. Exp. Med.* 208:1377–1388. http://dx.doi.org/10.1084/jem.20102065

Legge, K.L., and T.J. Braciale. 2003. Accelerated migration of respiratory dendritic cells to the regional lymph nodes is limited to the early phase of pulmonary infection. *Immunity.* 18:265–277. http://dx.doi.org/10.1016/S1074-7613(03)00023-2

Linterman, M.A., and C.G. Vinuesa. 2010. Signals that influence T follicular helper cell differentiation and function. *Semin. Immunopathol.* 32:183–196. http://dx.doi.org/10.1007/s00281-009-0194-z

Morita, R., N. Schmitt, S.E. Bentebibel, R. Ranganathan, L. Bourdery, G. Zurawski, E. Foucat, M. Dullaers, S. Oh, N. Sabzghabaei, et al. 2011. Human blood CXCR5(+)CD4(+) T cells are counterparts of T follicular cells and contain specific subsets that differentially support antibody secretion. *Immunity.* 34:108–121. http://dx.doi.org/10.1016/j.immuni.2010.12.012

Nurieva, R.I., Y. Chung, D. Hwang, X.O. Yang, H.S. Kang, L. Ma, Y.H. Wang, S.S. Watowich, A.M. Jetten, Q. Tian, and C. Dong. 2008. Generation of T follicular helper cells is mediated by interleukin-21 but independent of T helper 1, 2, or 17 cell lineages. *Immunity.* 29:138–149. http://dx.doi.org/10.1016/j.immuni.2008.05.009

Nurieva, R.I., Y. Chung, G.J. Martinez, X.O. Yang, S. Tanaka, T.D. Matskevitch, Y.H. Wang, and C. Dong. 2009. Bcl6 mediates the development of T follicular helper cells. *Science.* 325:1001–1005. http://dx.doi.org/10.1126/science.1176676

Pelletier, N., L.J. McHeyzer-Williams, K.A. Wong, E. Urich, N. Fazilleau, and M.G. McHeyzer-Williams. 2010. Plasma cells negatively regulate the follicular helper T cell program. *Nat. Immunol.* 11:1110–1118. http://dx.doi.org/10.1038/ni.1954

Schaerli, P., K. Willimann, A.B. Lang, M. Lipp, P. Loetscher, and B. Moser. 2000. CXC chemokine receptor 5 expression defines follicular homing T cells with B cell helper function. *J. Exp. Med.* 192:1553–1562. http://dx.doi.org/10.1084/jem.192.11.1553

Sun, J., R. Madan, C.L. Karp, and T.J. Braciale. 2009. Effector T cells control lung inflammation during acute influenza virus infection by producing IL-10. *Nat. Med.* 15:277–284. http://dx.doi.org/10.1038/nm.1929

Sun, J., H. Dodd, E.K. Moser, R. Sharma, and T.J. Braciale. 2011. CD4+ T cell help and innate-derived IL-27 induce Blimp-1-dependent IL-10 production by antiviral CTLs. *Nat. Immunol.* 12:327–334. http://dx.doi.org/10.1038/ni.1996

Sundararajan, A., L. Huan, K.A. Richards, G. Marcelin, S. Alam, H. Joo, H. Yang, R.J. Webby, D.J. Topham, A.J. Sant, and M.Y. Sangster. 2012. Host differences in influenza-specific CD4 T cell and B cell responses are modulated by viral strain and route of immunization. *PLoS ONE.* 7:e34377. http://dx.doi.org/10.1371/journal.pone.0034377

Topham, D.J., R.A. Tripp, A.M. Hamilton-Easton, S.R. Sarawar, and P.C. Doherty. 1996. Quantitative analysis of the influenza virus-specific CD4+ T cell memory in the absence of B cells and Ig. *J. Immunol.* 157:2947–2952.

Vinuesa, C.G., S.G. Tangye, B. Moser, and C.R. Mackay. 2005. Follicular B helper T cells in antibody responses and autoimmunity. *Nat. Rev. Immunol.* 5:853–865. http://dx.doi.org/10.1038/nri1714

Vogelzang, A., H.M. McGuire, D. Yu, J. Sprent, C.R. Mackay, and C. King. 2008. A fundamental role for interleukin-21 in the generation of T follicular helper cells. *Immunity*. 29:127–137. http://dx.doi.org/10.1016/j.immuni.2008.06.001

Waffarn, E.E., and N. Baumgarth. 2011. Protective B cell responses to flu—no fluke! *J. Immunol.* 186:3823–3829. http://dx.doi.org/10.4049/jimmunol.1002090

Yoo, J.K., D.P. Baker, and E.N. Fish. 2010a. Interferon-β modulates type 1 immunity during influenza virus infection. *Antiviral Res.* 88:64–71. http://dx.doi.org/10.1016/j.antiviral.2010.07.006

Yoo, J.K., C.L. Galligan, C. Virtanen, and E.N. Fish. 2010b. Identification of a novel antigen-presenting cell population modulating antiinfluenza type 2 immunity. *J. Exp. Med*. 207:1435–1451. http://dx.doi.org/10.1084/jem.20091373

Yusuf, I., R. Kageyama, L. Monticelli, R.J. Johnston, D. Ditoro, K. Hansen, B. Barnett, and S. Crotty. 2010. Germinal center T follicular helper cell IL-4 production is dependent on signaling lymphocytic activation molecule receptor (CD150). *J. Immunol.* 185:190–202. http://dx.doi.org/10.4049/jimmunol.0903505

Zaretsky, A.G., J.J. Taylor, I.L. King, F.A. Marshall, M. Mohrs, and E.J. Pearce. 2009. T follicular helper cells differentiate from Th2 cells in response to helminth antigens. *J. Exp. Med*. 206:991–999. http://dx.doi.org/10.1084/jem.20090303